High-accuracy height differences using a pressure sensor for ground control points measurement in underwater photogrammetry

High-accuracy height differences using a pressure sensor for ground control points measurement in underwater photogrammetry

Fabio Menna [1], Erica Nocerino [2], Alessio Calantropio [2]

[1] Department of Chemical, Physical, Mathematical and Natural Sciences, University of Sassari, Sassari, Italy – fmenna@uniss.it
[2] Department of Humanities and Social Sciences, University of Sassari, Sassari, Italy; Email: (enocerino; acalantropio)@uniss.it

Commission II/WG7

Keywords: underwater photogrammetry, pressure sensor, depth measurement, ground control points, low-cost sensor.

Abstract:

Three-dimensional reference points (RPs) are fundamental for datum definition and metric validation in many photogrammetric applications, often used as ground control points (GCPs) to constrain the bundle adjustment solution. Nevertheless, survey operations underwater present challenges due to the physical characteristics of the water itself and the technological limitations of available instruments. Traditional methods to collect RPs underwater rely on direct geodetic measurements like slope distances, height differences, and depths from a dive computer. These methods can be time-consuming and impractical to scale up to large areas, particularly in deeper waters. This paper reports on the use of a custom-developed low-cost pressure sensor to measure depths and height differences of underwater RPs with survey-grade accuracy. Laboratory and open water tests demonstrated the method's potential, achieving an $RMSE_Z$ of less than 1 mm over a 1.5 m height range in the laboratory in static water and a sub-centimetre RMSE of relative depth differences in shallow water tests carried out in two different locations at sea with maximum significant wave height of 9 cm. The sensor proved its effectiveness also for constraining a corridor-like underwater photogrammetric survey reducing the bending of the 3D model with respect to the free network solution ($RMSE_Z$ lowered from 10 cm to less than 1 cm). The preliminary tests with the presented approach proved several advantages against other consolidated methods, including cost reduction (compared to commercial survey instruments), rapidity, safety, and accuracy, especially at depths greater than 3-5 m where other approaches (e.g., GNSS or topographic measures) cannot be applied.

1. Introduction

Photogrammetry may enable effective mapping and monitoring of the underwater environment; however, this is subject to the implementation of reliable georeferencing strategies for ensuring that all the resulting products are co-registered within a common reference system.

Three-dimensional points of known coordinates are a common form of reference used in photogrammetry both for datum definition (i.e., scaling, rotation, and translation), constraining the bundle adjustment solutions (ground control points, GCPs), and independent check of metric validation (i.e., check points, CPs). Above the water, the collection of reference points (RPs) is a conventional, relatively inexpensive, and easy-to-implement practice, particularly when leveraging the latest geodetic surveying instruments and methods (i.e., multi-constellation geodetic GNSS receivers, robotized total stations – TS, IMU-based tilt compensation for pole-based measurements). On the other hand, when it comes to the underwater environment, technology has not yet reached a similar level of maturity, or, in some cases, it simply does not exist at all. In fact, in contrast to terrestrial environments where traditional geodetic surveying techniques are well established, their direct application in water is significantly limited. The main obstacle is the limited availability of satellite signals from Global Navigation Satellite Systems (GNSS), including GPS, as electromagnetic waves are attenuated considerably by water, making them unusable for positioning applications in underwater assets.

The most common surveying method of three-dimensional control in underwater photogrammetry, especially in shallow water (less than 30 m for SCUBA divers), relies on direct measurement of distances using tape meters and depths from dive computers (Rule, 1989). In archaeological topographic surveys, the trilateration method using a tape measure is common, with an average error varying from 1 cm (Rule, 1989) to 5 cm (Balletti et al., 2015), depending on the length of the measured slope distance.

Nocerino et al. (2020) and Lo et al. (2024) collected sub-centimetric accuracy GCPs for photogrammetric multitemporal analysis in ecological research applications. Direct measurements by SCUBA divers were carried out using tape measurements for distances and geometric levelling for depth differences. The geometric levelling used an underwater laser mounted on a tripod and a level staff. Despite the high accuracy, the greater complexity of these underwater surveys carried out by divers restricts their use only to areas of limited extension and at shallow depths (< 20 m).

Traditional archaeological excavation methods, especially in underwater environments, often rely on scale bars or approximate topographic measurements. Scale bars can solve the scale ambiguity of the photogrammetric model and its derived products; however, they do not provide either absolute georeferencing or guarantee that the model is not deformed due to the presence of uncompensated systematic errors.

Professional saturation divers and ROVs used special extensible wires in deeper waters to measure distances for Oil&Gas applications (IMCA, 2017). These direct measurements are then adjusted to provide three-dimensional coordinates of RPs using standard least square procedures where each observation equation is weighted according to its precision. The most critical part of these approaches relates to the determination of the Z

coordinate because of the uncertainty in measuring the depth, primarily due to the low accuracy of standard diving computers and the effect of sea surface conditions. For this reason, these types of surveys are not well suited for high-accuracy control (Skarlatos et al., 2019).

In recent years, advances have been made in underwater communication and positioning devices that use acoustic signals on short baselines (USBL). Still, their accuracy is in the order of a few decimetres for short distances (below 100 m). Therefore, they are mainly suitable for navigation purposes and approximate georeferencing but not for controlling high-resolution underwater photogrammetry surveys (Krzysztof & Aleksander, 2016).

In very shallow waters (< 5 m), the use of high-precision differential GNSS measurements such as RTK or PPK methods was tested using a special prototype consisting of a buoy with an extensible rod connected to a tilt sensor (Reich et al., 2021). A more classic rod kept vertical in Balletti et al. (2015) or a 2 m high tripod (Wright et al., 2020) were also employed. More recently, Calantropio and Chiabrando (2024) showed that using a tilt-compensated GNSS receiver virtually removes the need to keep the rod vertical during the measurement, resulting in a much higher potential accuracy and efficiency of the method, but provided that the rod does not bend during the survey, for example, due to the effect of waves or strong wind. Although tilt-compensated GNSS receivers may provide an effective solution for measuring RPs in very shallow waters, measuring height differences with centimetric accuracy in waters deeper than 5 m may be unfeasible with this technology.

Topographic surveys of submerged points in shallow waters using a total station (TS) ashore are also possible, but with an unobstructed line of sight between the total station and the measured RPs and limited to the pole length used. In very shallow waters, classic surveying with TS from shore can provide an efficient solution to measure a reference network with centimetre accuracy, if divers holding the pole in water ensure prism verticality. However, inherent limitations exist, such as environmental conditions affecting the pole's stability, worsening the achievable accuracy (Calantropio and Chiabrando, 2024). Nowadays, surveying tilt-compensated poles are available on the market, which may help reduce these adverse effects, as in the case of the tilt-compensated GNSS receiver (Smouha, 2019).

This manuscript presents an experimental study for measuring height differences underwater with a prototype pressure sensor (PS) device developed by the authors (Menna et al., 2021). The PS provided pressure measurements to transform an underwater photogrammetric network in a local vertical reference frame, providing the four degrees of freedom with scaling, levelling (two angles), and vertical translation. In this contribution, the same PS is tested as a device for measuring both absolute depths and relative height differences between underwater RPs.

2. Depth determination from hydrostatic pressure

At a specific depth *D* underwater, the pressure *P* exerted by the water at equilibrium is:

$$P = P_0 + \rho g D \tag{1}$$

$$D = \frac{P - P_0}{\rho g} \tag{2}$$

Where the product ρg, i.e. density of water multiplied by the gravitational acceleration, is called "specific weight" and can be considered constant for a given location underwater (if temperature and salinity do not change); P_0 is the atmospheric pressure measured at the water surface. ρ and g can be determined experimentally measuring the volume and the mass of a water sample in laboratory for density measurement and a gravimeter for the gravitational acceleration g. Approximations in the order of 1 ‰ could be obtained using normal gravity formulas or tables. Temperature and salinity of the water need to be considered for the density, while latitude and elevation (for example, in the case of a mountain lake) are the most important parameters influencing g.

Equations (1-2) holds for waters at equilibrium. It must be noted that the depth *D* of a point on the sea bottom using equation (2) varies with time depending on tides and waves, which rise or lower the water surface level, and based on weather conditions, in particular the atmospheric pressure, thus directly affecting the measurement of P_0. Since these effects typically happen in a time frame of hours, they can be considered negligible or mitigated by measuring relative depth differences between two points ΔD_{12} (equal to the inverse of their height difference ΔH_{12}) in a time span such that P_0 can be considered constant and is eliminated:

$$\Delta D_{12} = -\Delta H_{12} = \frac{P_2 - P_1}{\rho g} \tag{3}$$

The relations between the variables and the constants introduced in equations (1-3) is visually represented in Figure 1.

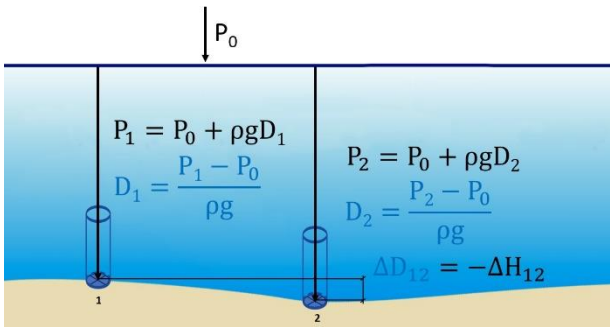

Figure 1. Depth differences between two points as measured with the PS.

2.1 Laboratory tests using a self-made pressure chamber

A newer version of the PS presented in Menna et al. (2021) was immersed in a self-made pressure chamber (Figure 2), a sealed transparent encloser filled with tap water (temperature of about 15 °C) and connected to a transparent hose, open to ambient pressure. With this setup, raising or lowering the hose changes the height of the water column and thus the exerting pressure inside the chamber.

We then placed a measuring tape vertically on a wall and then moved the hose raising or lowering the water surface level to 16 different heights 10 cm apart. The PS was triggered at each height level of the hose via optical signals from outside the pressure chamber. The pressure was recorded for about 10 seconds at about 4 Hz. For each height, the average pressure was computed and then converted to depth using $\rho = 997.8\ kg/m^3$ and $g = 9.8031\ m/s^2$, nominal values taken from water density tables and the Italian gravimetric map, respectively.

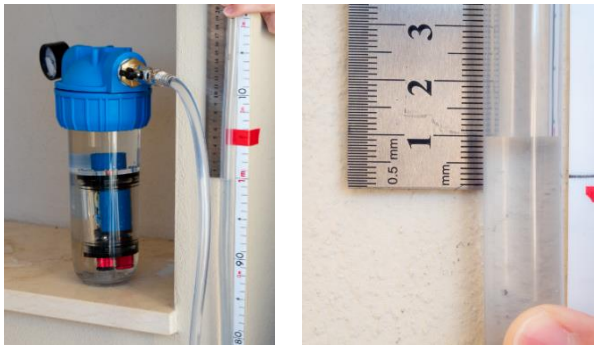

Figure 2. Hydrostatic pressure measurements in the laboratory to experimentally evaluate the accuracy of the PS.

We then fitted a regression line (Figure 3) between the measured depths from the pressure sensor and the readings on the measuring tape fixed on the wall, which were considered our reference measurements. This calibration procedure allows understanding whether a residual scale factor exists between the two sets of depths and eliminates the vertical offset. The linear correlation coefficient shows an almost exact linearity (up to the 4th decimal place) with an RMS of residuals of less than 1 mm over a maximum delta height of 1.5m. The slope m provides a scale factor between the measured and reference heights, thus indicating if the measured heights are systematically larger or smaller. A value significantly different from 1 could highlight a wrong estimation of the specific weight ρg.

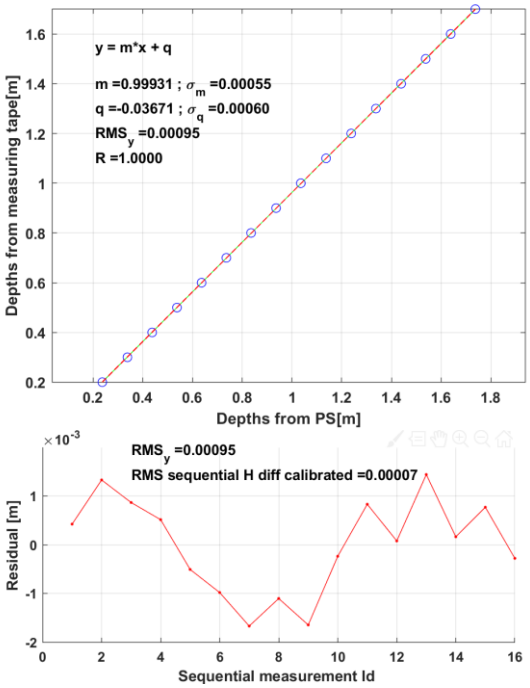

Figure 3. Up: Linear fitting of the pressure sensor depths vs reference depths from a measuring tape (the values are expressed in meters). Down: Residuals of the linear fitting shown above. Values correspond to the sequential order of the depth measurements. A sinusoidal pattern can be observed, suggesting a temporal correlation between measurements.

The temporal distribution of the measurement residuals shows a sinusoidal pattern (Figure 3 down) and exhibits a strong temporal correlation. To assess the PS potential in measuring relative height differences underwater, depth differences (every 10 cm) between subsequent observations were computed and compared with the same differences from reference measurements. The RMS of differences between the two sets of measurements is 0.07 mm, corresponding to a relative height error of about 1:1450.

2.2 Shallow water tests

We performed two measurement campaigns in two different locations at sea in Sardinia, Italy, about 30 km apart from each other in open shallow water (maximum depth of about 1.6 m). For both cases we used $\rho = 1028.9\ kg/m^3$ and $g = 9.8031\ m/s^2$, also in this case nominal values. With respect to the laboratory test in the two real-word experiments, the depth measurements obtained using the PS depth measurements were compared against the heights measured with a total station (TS). The PS was attached to a geodetic pole mounting a prism, tracked with the total station (Figure 4).

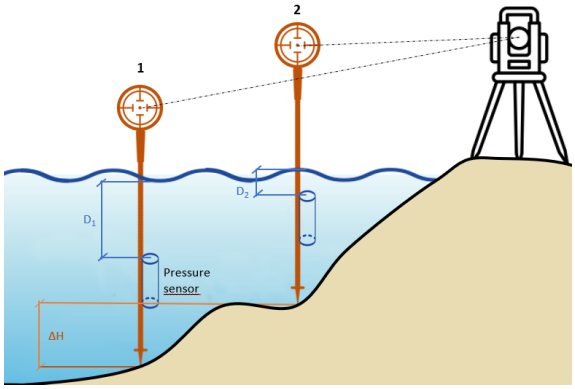

Figure 4. Experimental evaluation of the developed pressure sensor in measuring height differences at sea. Accuracy evaluation tests using a prism tracked by a TS in shallow water.

For each point, the pole was kept still in the position to measure for a minimum of 90 seconds, during which the PS logged the depths at 4 Hz while the TS operator repeated several measurements of the prism. The chosen 90-second measurement duration was expected to be longer than the maximum wavelength period in the area during the tests. In both cases, the pressure P_0 was measured with the pressure sensor before and at the end of the experiments to ensure that possible drift was accounted for during data processing. The assumption is that a regular sea state is the sum of several sinusoidal waves and that averaging the heights over a long period would significantly reduce their effect as if the sea was in static conditions (Figure 5).

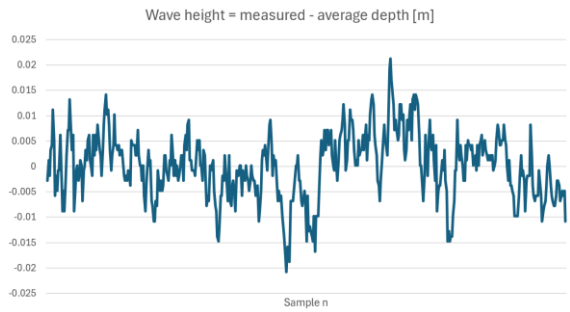

Figure 5. An example of recorded wave heights over 90 seconds in a static position of the PS. The average significant wave height is about 3 cm.

2.2.1 Depth measurement in the Bay of Porto Conte: The first experiment was conducted in the bay of Porto Conte (Figure 6 up); the weather was characterized by strong wind gusts, but the water was calm because of the closed bay that did not allow waves to form (Figure 7). The water temperature was about 14 °C. The pole was positioned at 22 different points, spanning a depth range of about 1.1 m. Figure 5 reports an example of the logged depths in one location as recorded by the pressure sensor rigidly attached to the pole and kept static. The graph shows the whole waveform with a significant wave height of about 3 cm. The measurement of the 22 different points lasted about one hour, with an average of 1.5 minutes for the depth measurement and 1.5 minutes to reach each new location.

Figure 6. Up: The area of the very shallow calm water test in the Porto Conte location (Sardinia, Italy). The yellow triangle represents the position of the TS, while the red circle symbolizes the area in which the RPs were measured. Down: the TS operator measures the prism on the pole, held vertically in the water and which the PS is mounted on.

Similarly to laboratory measurements, a regression line was estimated, showing this time a greater RMSE of about 2.1 cm and maximum residuals of about 3 cm. Also, the slope m in this case resulted different from unity of about 12 ‰ with a standard deviation of the slope of 15 ‰. (Figure 7 up). As highlighted in the laboratory test, the residual graph showed a temporal dependency of the residuals. By comparing the relative depth differences from the PS and the TS between subsequent depth measurements, the RMS results equal to 6 mm (Figure 7 down).

2.2.2 Depth measurements at Ezzi Mannu: A second test was conducted on the shore of Ezzi Mannu. The acquisition lasted 70 minutes (Figure 8 up), and 22 points were measured. Eight were distributed over a corridor pattern about 50 m long and 2 m wide, materialized with targets (Figure 8 down), and used for the photogrammetric test presented in subsection 2.2.3. The water temperature was 14 °C.

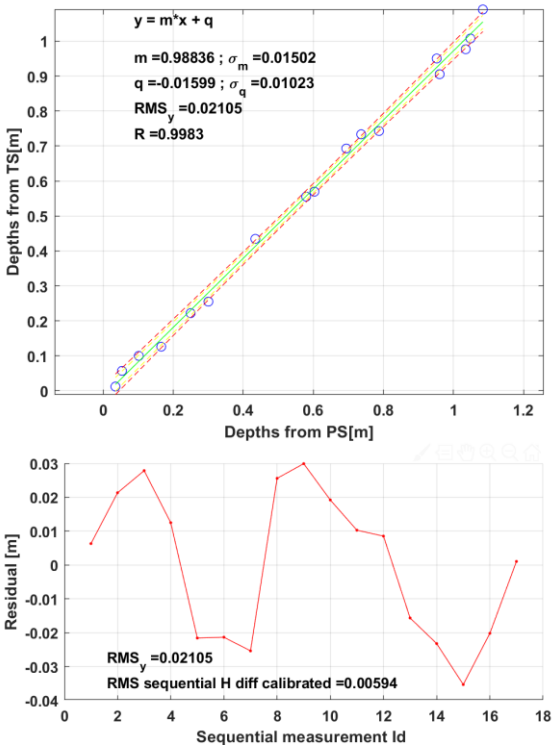

Figure 7. Up: Linear fitting and related confidence region (3 sigma) of the PS depth measurements vs. reference depths from TS in the Bay of Porto Conte (values are expressed in meters).)Down: Residuals of the linear fitting shown above. Values correspond to the sequential order of the depth measurements.

Figure 8. Up: Depth measuremnet campain at Ezzi Mannu: while the TS tracks the prism, the operator keeps the pole with the PS rigidly attached vertical. Down: the area of the very shallow water test in Ezzi Mannu Beach (Sardinia, Italy). The yellow triangle represents the position of the TS, while the black and white markers symbolize the positions of the measured targets..

Repeated depth measurements of the same points resulted in an RMS of 3.6 mm, providing an estimate of the repeatability of the procedure. Analogously to the other case studies, Figure 9 up reports the regression line for the depth measurements at the Ezzi Mannu test site. The RMS of residuals is about 8.5 mm for the absolute depths and 2.3 mm when considering the relative depth differences (Figure 9 down). From the depth recordings, the average significant wave height resulted about 9 cm. .

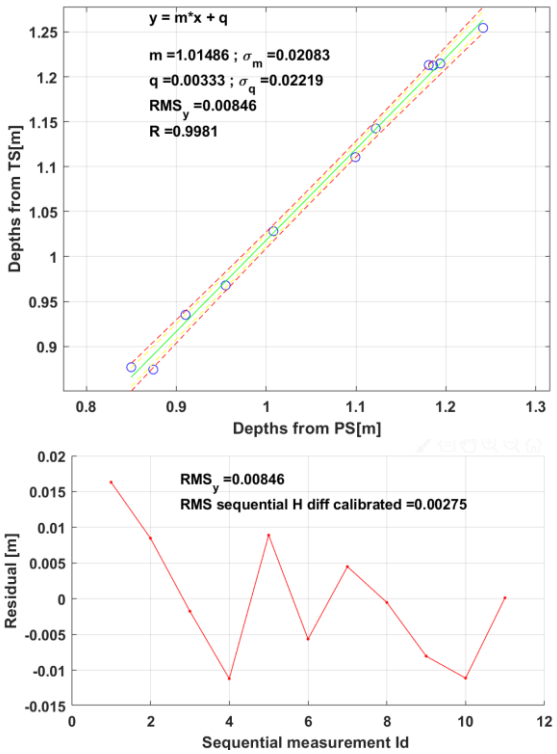

Figure 9. Up: Linear fitting and related confidence region (3 sigma) of the pressure sensor depths measurements vs reference depths from TS at the beach of Ezzi Mannu (values are expressed in meters). Down: Residuals of the linear fitting shown above. Values correspond to the sequential order of the depth measurements.

2.2.3 Corridor mapping with underwater photogrammetry and depth constraints: Open water photogrammetry tests were realized to demonstrate the benefits of depth measurements used as height ground control in real-word applications. The rationale behind the experiment is that when working with weak camera network configurations and self-calibrating bundle adjustment in a structure from motion approach, 3D deformations are likely to occur, resulting in a typical bending of the reconstructed 3D model (Nocerino et al., 2014; Menna et al 2020; James and Robson, 2014). These deformations are more prominent along the vertical direction, therefore, by constraining the bundle adjustment solution using the depths of the targets measured with the PS, their magnitude should reduce. The 3D model would, in fact, follow the ground control, thus increasing its geometric accuracy. Moreover, the use of depth measurements not only provides a vertical datum (vertical translation) to the resulting 3D model, but it also solves for its orientation (vertical direction or levelling with two angles), thus solving three degrees of freedom.

A 50 m long corridor-like image acquisition was then performed in the presented test site (Figure 8 up). A 20 MP Olympus OM-D E-M1 Mark II Micro Four Thirds camera with a Panasonic Lumix 8mm fisheye lens in an Olympus PT-EP14 waterproof housing mounting a dome port was used to acquire about 1000 images with a GSD of about 0.4 mm in a single strip with an almost downward-looking nadiral camera network (Figure 10 a, b).

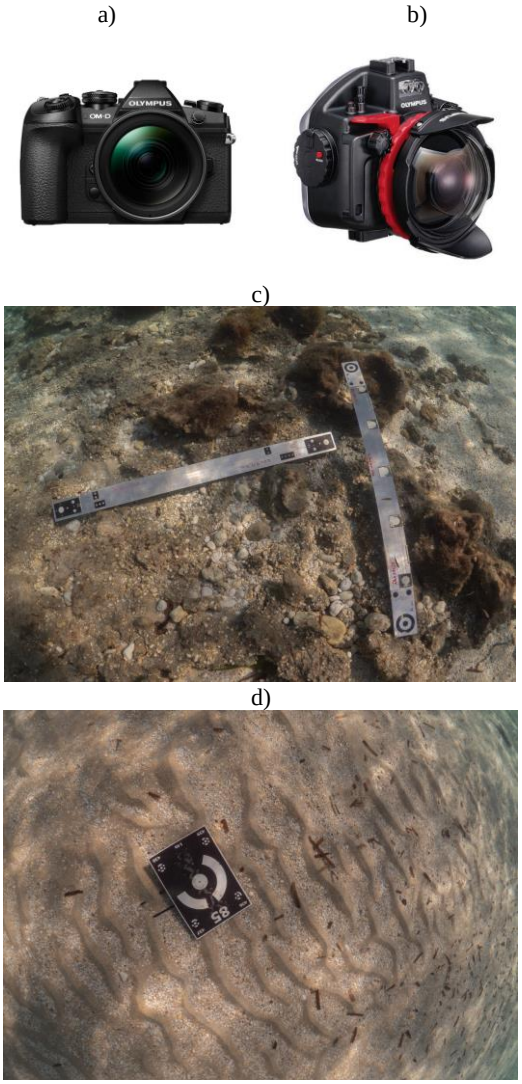

Figure 10. Olympus OM-D E-M1 mark II (a) and waterproof housing PT-EP14 with dome port (b) used for the underwater photogrammetry test along with two sample photographs showing the aluminum scale bars (c) and one of the measured targets (d). Water caustics are also visible.

This acquisition reproduces a weak camera geometry, which usually leads to very deformed 3D models due to uncompensated residual systematic errors not properly modelled in self-calibrating processing. The sea bottom was mainly flat and covered by sand and scattered stones. Two 1 m long aluminium (Figure 10 c) scale bars were positioned in the middle of the strip and used for scaling. Water caustics were visible (Figure 10 c, d) but did not negatively affect the image orientation stage.

The photogrammetric acquisition was processed in Agisoft Metashape[1] (Figure 11 a) both in a free network and in a constrained bundle adjustment using the depths of the eight targets measured with the PS. The 3D coordinates of the same targets, measured with the TS, were used to assess the empirical accuracy. In both cases, the two scale bars were used for scaling.

For the free network adjustment, although the residuals on the scalebars were lower than 0.15 mm, the vertical error $RMSE_Z$ on RPs from TS showed a strong bending with vertical errors greater than 0.25 m (Figure 11 b). Using the scalebars for scaling and the depths from the PS to constrain the bundle adjustment, the $RMSE_Z$ was lowered from about 10 cm of the free network solution to 6 mm.

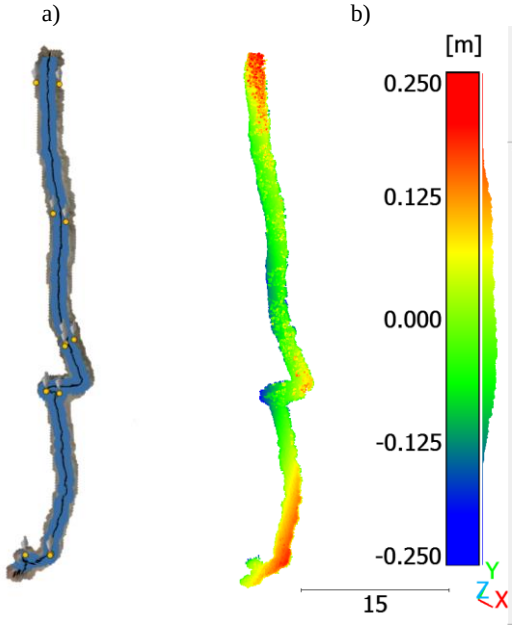

Figure 11. Underwater corridor surveyed with a single nadiral strip. The resulting camera network is in blue, with targets (a) and Euclidean distances (b) between the free network solution and the reference 3D model obtained using the TS RPs as GCPs in the bundle adjustment.

3. Conclusions

Following the need for precise underwater georeferencing approaches, this study outlined the potential application of a novel PS for surveying RPs functional to the photogrammetric acquisition of submerged environments. Detailed procedures for experimental tests of the PS, both in the laboratory and on-site, showed its potential benefits in underwater photogrammetry applications.

The preliminary results proved that the method has significant advantages in terms of speed, safety, ease of use, and accuracy compared to traditional geodetic methods for RPs measurements used in underwater photogrammetry at depths greater than 3-5 m.

The laboratory tests showed an accuracy better than 1 mm when the water is at an equilibrium state. Open water tests showed that even in presence of a significant wave height of about 9 cm, sub-centimetre accuracy could be achieved in measuring both absolute depths and relative depth differences. In the Porto Conte test, the absolute depths resulted less accurate than in the Ezzi Mannu experiment, despite the lower average significant wave height (3cm versus 9cm). Most likely, the presence of strong wind gusts in a closed bay resulted in waves with an average longer period than the 90 seconds used for recording each depth. Indeed, the use of the sensor in a differential way to compute the relative height differences showed a significant improvement of the accuracy (from 21mm to 6). We will further investigate this aspect in the future.

In the current experiments in open water, each depth measurement took, on average, about 2 minutes to mitigate the effect of waves. This time duration could be shortened or increased depending on the local sea state conditions.

The proposed depth measurements can be used both in an underwater geodetic survey approach along with trilateration to provide high accuracy and vertical control faster than laser-based geometric levelling or used, as shown in subsection 2.2.3, to constrain photogrammetric bundle adjustment solutions. In the presented scenario, the experimental results proved that using scale bars and depths from the pressure sensor as constraints in the bundle adjustment improves the accuracy of the image orientation with sub-centimetre $RMSE_Z$.

Given the challenges and constraints related to underwater survey operations, the presented methodology based on the PS can ease complex georeferencing surveying procedures, facilitating the scientific documentation, mapping, and monitoring of the underwater environment.

Acknowledgments

This research was supported by: MANATEE - Monitoring and mApping of mariNe hAbitat with inTegrated gEomatics technologiEs (J53D23002570001) PRIN 2022-2024 project, funded by the European Union, Next Generation EU, and POSEIDON - multitemPOral SEagrass mapping and monitoring of posIDONia meadows and banquettes for blue carbon conservation (E53D23021870001), a research project of Italian national relevance initiative "Italia Domani - Piano Nazionale di Ripresa e Resilienza" (PNRR) funded by the European Commission - Next Generation EU. EN acknowledges the support of NBFC to University of Sassari, funded by the Italian Ministry of University and Research, PNRR, Missione 4 Componente 2, "Dalla ricerca all'impresa", Investimento 1.4, Project CN00000033.

References

Balletti, C., Beltrame, C., Costa, E., Guerra, F., and Vernier, P. 2015. Underwater Photogrammetry And 3d Reconstruction Of Marble Cargos Shipwreck, Int. Arch. Photogramm. Remote Sens. Spatial Inf. Sci., XL-5/W5, 7–13, https://doi.org/10.5194/isprsarchives-XL-5-W5-7-2015.

Calantropio, A. and Chiabrando, F., 2024. Georeferencing Strategies in Very Shallow Waters: A Novel GCPs Survey Approach for UCH Photogrammetric Documentation. Remote Sensing, 16(8), p.1313.

IMCA, International Marine Contractors Association, "Guidance on subsea metrology," IMCA S 019, 2017. https://www.imca-int.com/publications/318/guidance-on-subsea-metrology/

[1] https://www.agisoft.com/

Krzysztof, N. and Aleksander, N., 2016. The positioning accuracy of BAUV using fusion of data from USBL system and movement parameters measurements. Sensors, 16(8), p.1279.

James, M.R. and Robson, S., 2014. Mitigating systematic error in topographic models derived from UAV and ground-based image networks. Earth Surface Processes and Landforms, 39(10), pp.1413-1420.

Lo, E., Lozano Bravo, H., Hui, N., Nocerino, E., Menna, F., Rissolo, D., Kuester, F. 2024. Evaluation of the Accuracy of Photogrammetric Reconstruction of Bathymetry Using Differential GNSS Synchronized with an Underwater Camera. Int. Arch. Photogramm. Remote Sens. Spatial Inf. Sci., *On Press*.

Menna, F., Nocerino, E., Ural, S. and Gruen, A., 2020. Mitigating image residuals systematic patterns in underwater photogrammetry. Int. Arch. Photogramm. Remote Sens. Spatial Inf. Sci., 43, pp.977-984.

Menna, F., Nocerino, E., Chemisky, B., Remondino, F. and Drap, P., 2021. Accurate scaling and levelling in underwater photogrammetry with a pressure sensor. c43, pp.667-672.

Nocerino, E., Menna, F., Gruen, A., Troyer, M., Capra, A., Castagnetti, C., Rossi, P., Brooks, A.J., Schmitt, R.J. and Holbrook, S.J., 2020. Coral reef monitoring by scuba divers using underwater photogrammetry and geodetic surveying. Remote Sensing, 12(18), p.3036.

Nocerino, E., Menna, F. and Remondino, F., 2014. Accuracy of typical photogrammetric networks in cultural heritage 3D modeling projects. Int. Arch. Photogramm. Remote Sens. Spatial Inf. Sci., 40, pp.465-472.

Reich, J., Steiner, P., Ballmer, A., Emmenegger, L., Hostettler, M., Stäheli, C., Naumov, G., Taneski, B., Todoroska, V., Schindler, K. and Hafner, A., 2021. A novel structure from motion-based approach to underwater pile field documentation. Journal of Archaeological Science: Reports, 39, p.103120.

Rule, N., 1989. The Direct Survey Method (DSM) of underwater survey, and its application underwater. International Journal of Nautical Archaeology, 18(2), pp.157-162.

Skarlatos, D., Menna, F., Nocerino, E. and Agrafiotis, P., 2019. Precision potential of underwater networks for archaeological excavation through trilateration and photogrammetry. Int. Arch. Photogramm. Remote Sens. Spatial Inf. Sci., XLII-2/W10, 175–180.

Smouha, J., 2019. Independent Evaluation of the Leica GS18 T Tilt-Compensated GNSS RTK Rover. University of Southern Queensland, Faculty of Health, Engineering and Sciences. Bachelor Thesis

Wright, A.E., Conlin, D.L., Shope, S.M., 2020. Assessing the accuracy of underwater photogrammetry for archaeology: A comparison of structure from motion photogrammetry and real time kinematic survey at the East Key Construction Wreck. Journal of Marine Science and Engineering 8, 849. doi:10.3390/jmse8110849